Computational Engineering and Physical Modeling 1-2 (2018) 01-15

Contents lists available at **CEPM**

Computational Engineering and Physical Modeling

Journal homepage: www.jcepm.com

Transient Combustion Analysis for Iron Micro-Particles in a Gaseous Oxidizing Medium Using Adomian Decomposition Method

M.G. Sobamowo*, A.A. Yinusa

Department of Mechanical Engineering, University of Lagos, Nigeria

Corresponding author: *mikegbeminiyiprof@yahoo.com*

https://doi.org/10.22115/CEPM.2018.122052.1012

ARTICLE INFO

Article history:
Received: 09 March 2018
Revised: 06 May 2018
Accepted: 06 May 2018

Keywords:
Iron particle combustion;
Thermal radiation;
Temperature history;
Adomian decomposition method.

ABSTRACT

The present study presents analytical solution to transient combustion analysis for iron micro-particles in a gaseous oxidizing medium using Adomian decomposition method. The analytical solutions obtained by the Adomian decomposition method are verified with those of the fourth order Runge–Kutta numerical method. Also, parametric studies are carried out to properly understand the chemistry of the process and the associated burning time. Thermal radiation effect from the external surface of burning particle and variations of density of iron particle with temperature are considered. Furthermore, the results show that by increasing the heat realized parameter, combustion temperature increased until a steady state is reached. This work will be useful in solving to a great extent one of the challenges facing industries on combustion of metallic particles such as iron particles as well as in the determination of different particles burning time.

1. Introduction

The past few decades have experienced various industrial challenges associated with metallic particles combustion. Also, accurate prediction of the burning period of the combustibles has

How to cite this article: Sobamowo GM, Yinusa A. Transient Combustion Analysis for Iron Micro-Particles in a Gaseous Oxidizing Medium Using Adomian Decomposition Method. Comput Eng Phys Model 2018;1(2):1–15. https://doi.org/10.22115/cepm.2018.122052.1012

posed serious challenges to the transient analysis of the combustion process. Combustible dusts which approximates gaseous oxidizing media require an accurate knowledge of their explosion hazards in order to make their importance to manufacturing, generation, process and industrial application applaudable. As a result, researchers have ventured into better understanding and modeling the particle and dust combustion. In a recent study, Sun et al. [1] examined the combustion behavior of iron particles that is suspended in air. In their work, they considered the combustion zone propagating through an iron particle cloud and the combustion behavior of individual iron particles by using high-speed photomicrographs. They concluded that each iron particle combusts at the combustion zone without gas phase flame and the burn-out time is proportional to the diameter of iron particle when the particle diameter is not so large. Haghiri and Bidbadi [2] applied the principle of flame propagation to study the dynamic behavior of particles by considering a two-phase mixture which consists of micro-iron particles and air by considering the effect of thermal radiation. They obtained results which show that the considered thermal radiation plays a significant role in the improvement of vaporization process and burning velocity of organic dust mixture, compared with the case where this effect is correspondingly neglected. Liu et al. [3] adopted a combustion chamber as a space to investigate flame propagation through hybrid mixture of coal dust and methane under a standard atmosphere. A steady, uni-dimensional theoretical analysis of flame propagation mechanism through micro-iron dust particles based on dust particles' behavior with meticulous attention on the thermophoretic external forcing agent and under small Knudsen numbers is presented by Bidabadi et al. [4]. A mathematical model for studying and analyzing the structural properties of flame propagating through a two-phase mixture that consists of organic fuel particles and air is performed by Haghiri and Bidabadi [5]. They went further as compared to previous analytical studies by considering the thermal radiation effect which has not been attempted before. Recently, Hatami et al. [6] solved the nonlinear energy equation that resulted from Bidabadi and Mafi's work on particle combustion modeling [6] by applying the semi-analytical method, differential transformation method (DTM) and BPES. They flagged up equations for calculating the convective heat transfer coefficient and burning time especially for iron particles. Polynomial expansion methods (PEM) are widely used in many mathematical and engineering fields to ascertain vital results for both numerical and analytical analysis. Among the most frequently applied polynomials, weighted residual methods (WRMs) are one of the vital tools as a result of their simplicity and high accuracy when verified with other schemes. WRMs have examples which includes Galerkin, Collocation and least square. Stern et al. [7] used one of the examples of the WRMs called the collocation method for solving a third order linear differential equation. Vaferi et al. [8] have investigated the feasibility and continuity of applying of orthogonal collocation method to solve diffusivity equation in the radial unsteady flow system. Recently Hatami et al. [9] used collocation and Galerkin methods to study and perform heat transfer analysis through porous fins. The results obtained in the work was found to agree with existing ones. Aziz and Bouaziz [10,11] introduced least square method and used the method to obtain meaningful results for predicting the performance of longitudinal fins. It was later observed that least squares method is simple compared with some other analytical methods. Shaoqin and Huoyuan [12] obtained and used least-squares approximations for the constant density magneto-hydrodynamic equations also Hatami et al. [13–15], Hatami and Ganji [16–18], Hatami and

Domairry [19,20] and Ahmadi et al. [21] applied these analytical methods in different engineering problems. Saedodin and Shahababaei [22] applied homotopoy perturbation method (HPM) to study and analyze heat transfer in longitudinal porous fins while Darvishi et al. [23] and Moradi et al. [24] and Ha et al. [25] utilized homotopy analysis method (HAM) to obtain close form solution to the natural convection and radiation in a porous and porous moving fins. Also, Sobamowo et al. [26] applied homotopy perturbation method to analyze convective-radiative porous fin with temperature-dependent, internal heat generation and magnetic field. They presented interesting results and the validation of their work proves the efficiency of the scheme.

Adomian decomposition method (ADM) for solving linear and nonlinear differential equations has fast gained ground as it appeared in many engineering and scientific research papers [27–38]. It provides excellent approximations to the solution of non-linear equation with high accuracy. Therefore, in this work, Adomian decomposition method is applied to determine the temperature profile of iron particle during combustion. Parametric studies are carried out using the developed analytical solutions.

2. Problem description and governing equation.

Consider an iron spherical particle, Fig. (1) which is combusted in the gaseous oxidizing medium as a result of high reaction with oxygen which acts as an oxidizer.

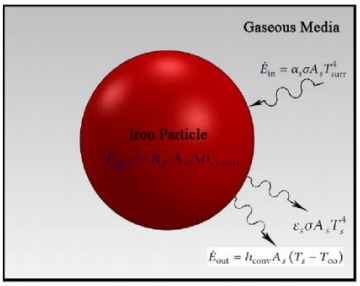

Fig. 1. Schematic of combusted iron particle in gaseous media (Hatami et al 2014).

The assumptions used includes:

(a) particle is considered to have constant temperature (Isothermal)

(b) the Biot number is small ($Bi << 0.1$)

(c) lumped system analysis is applied, ($T = T(t),\ T \neq T(r)$)

(d) the spherical particle combusts in an ambient medium.

(e) interactions with other particles is neglected.

(f) forced convection effect are neglected.

(g) constant thermo-physical properties for the particle and ambient gaseous oxidizer

(h) particle surface is assumed to be gray

(i) The surface reaction rate is treated as temperature independent with a constant convection heat coefficient.

By incorporating the above assumptions and performing energy balance:

$$\dot{E}_{in} - \dot{E}_{out} + \dot{E}_{gen} = \left(\frac{dE}{dt}\right)_p \tag{1}$$

where E_{in} is the rate at which energy enters the system as a result of the absorption of total radiation at the particle's surface from the environment, E_{out} is the rate at which energy leaves the system by convection mechanisms on the particle's surface and thermal radiation which emits from the outer surface of particle, E_{gen} is the rate of internal heat generation inside the particle due to the burning or combustion process and equals to the released heat from the chemical reaction, and (dE/dt) shows the rate of total energy changes in the particle. These energy terms may be represented as shown below:

$$\dot{E}_{in} = \alpha_s \sigma A_s T_{surr}^4 \tag{2}$$

$$\dot{E}_{out} = h_{conv} A_s \left(T_s - T_\infty\right) + \varepsilon_s \sigma A_s T_s^4 \tag{3}$$

$$\dot{E}_{gen} = \dot{Q}_{comb} = \dot{R}_p \, A_s \Delta h^o_{comb} \tag{4}$$

$$\left(\frac{dE}{dt}\right)_p = \rho_p V_p c_p \frac{dT_s}{dt} \tag{5}$$

By substituting the Eqs. (2) - (5) into Eq. (1),

$$\alpha_s \sigma A_s T_{surr}^4 - \left(h_{conv} A_s \left(T_s - T_\infty\right) + \varepsilon_s \sigma A_s T_s^4\right) + \dot{R}_p \, A_s \Delta h^o_{comb} = \rho_p V_p c_p \frac{dT_s}{dt} \tag{6}$$

In order to improve Eq. (6), the following assumptions are used:

(i) Kirchhoff's law is invoked, hence the surface absorptivity (α) and the emissivity (ε) at a given temperature and wavelength are equal.

(ii) Ignition temperature is used as the initial condition. ($T(0) = T_{ig}$)

(iii) Particle density is temperature dependent with a linear form that can be expressed as:

$$\rho_p = \rho_p\left(T\right) = \rho_{p,\infty}\left[1 + \beta\left(T - T_\infty\right)\right]$$

Applying the above assumptions, Eq. (6) becomes,

$$\rho_{p,\infty}\left[1 + \beta\left(T - T_\infty\right)\right] V_p c_p \frac{dT_s}{dt} + h_{conv} A_s \left(T_s - T_\infty\right) + \varepsilon_s \sigma A_s \left(T_s^4 - T_{surr}^4\right) - \dot{R}_p \, A_s \Delta h^o_{comb} = 0 \tag{7}$$

Introducing the following dimensionless parameters,

$$\begin{cases} \theta = \dfrac{T}{T_{ig}}, \quad \theta_{\infty} = \dfrac{T_{\infty}}{T_{ig}}, \quad \theta_{surr} = \dfrac{T_{surr}}{T_{ig}}, \quad \varepsilon_1 = \beta T_{ig} \\ \tau = \dfrac{t}{\left(\rho_{p,\infty} V_p c_p \Big/ h_{onv} A_s \right)}, \quad \psi = \dfrac{\dot{Q}_{comb}}{h_{conv} A_s T_{ig}}, \quad \varepsilon_2 = \dfrac{\varepsilon_s \sigma T_{ig}^3}{h_{conv}} \end{cases} \tag{8}$$

Using Eq. (8) in Eq. (7), the dimensionless form of Eq. (7) becomes,

$$\varepsilon_1 \theta \frac{d\theta}{d\tau} + \left(1 - \varepsilon_1 \theta_{\infty}\right) \frac{d\theta}{d\tau} + \varepsilon_1 \left(\theta^4 - \theta_{surr}^4\right) + \theta - \psi - \theta_{\infty} = 0, \tag{9}$$

with initial condition,

$$\theta(0) = 1. \tag{10}$$

3. Principle of adomian decomposition method

The principle of the method is described as follows. The general nonlinear equation is in the form

$$Lu + Ru + Nu = g \tag{11}$$

The linear terms are decomposed into $L + R$, with L taken as the highest order derivative which is easily invertible and R as the remainder of the linear operator of less order than L. where g is the system input or the source term and u is the system output, Nu represents the nonlinear terms, which is assumed to be analytic. $L^{-1}$is regarded as the inverse operator of L and is defined by a definite integration from 0 to x, i.e.

$$[\mathrm{L}^{-1} f](x) = \int_0^x f(v) dv \tag{12}$$

If L is a second-order operator, then L^{-1} is a two ford indefinite integral i.e. L^{-1} could be expressed as

$$[\mathrm{L}^{-1} f](x) = \int_1^x \int_0^x f(v) dv dv \tag{13}$$

Applying the inverse operator $L^{-1}$to the both sides of Eq. (11), and using the given conditions, the resulting equation could be written as

$$u = \mu(x) - L^{-1} Ru - L^{-1} Nu \tag{14}$$

Where $\mu(x) = \lambda_x + L^{-1} g$ and λ_x represents the term arising from integrating the source term g(x).

The Adomian methods decomposes the solution u(x) into a series

$$u = \sum_{m=0}^{\infty} u_m \tag{15}$$

and the nonlinear term into a series

$$Nu = \sum_{m=0}^{\infty} A_m \tag{16}$$

Where A_m's are Adomian's polynomials of $u_0, u_1, \ldots, u_m$ and are obtained for the nonlinearity $Nu = f(u)$ from the recursive formula

$$A_m = \frac{1}{m!}\left[\frac{d^m}{d\zeta^m}[\, fu(\zeta)]\right]_{\zeta=0} = \frac{1}{m!}\left[\frac{d^m}{d\zeta^m} f\left(\sum_{i=0}^{\infty}\zeta^i y_i\right)\right]_{\zeta=0} \qquad m = 0,1,2,3,\ldots \tag{17}$$

Where ζ is a grouping parameter of convenience.

The Adomian decomposition method defines the solution of the function $f(x)$ to be approximated as

$$f(x) = \sum_{m=0}^{\infty} f_m(x) \tag{18}$$

Applying the principle of ADM to Eq. (5), we have

$$\theta = -\left(\frac{\varepsilon_1}{1-\varepsilon_1\theta_\infty}\right)L^{-1}\theta\frac{d\theta}{d\tau} - \left(\frac{\varepsilon_2}{1-\varepsilon_1\theta_\infty}\right)L^{-1}\theta^4 - \left(\frac{1}{1-\varepsilon_1\theta_\infty}\right)L^{-1}\theta + L^{-1}\left(\frac{\psi+\theta_\infty+\varepsilon_2\theta_{surr}^4}{1-\varepsilon_1\theta_\infty}\right) \tag{19}$$

where $L^{-1} = \int_0^{\tau}(\bullet)d\tau$

Grouping and re-representing the coefficients,

$$\theta = \beta_1 L^{-1}\theta\frac{d\theta}{d\tau} + \beta_2 L^{-1}\theta^4 + \beta_3 L^{-1}\theta + L^{-1}\beta_4 \tag{20}$$

where

$$\beta_1 = -\left(\frac{\varepsilon_1}{1-\varepsilon_1\theta_\infty}\right),\quad \beta_2 = -\left(\frac{\varepsilon_2}{1-\varepsilon_1\theta_\infty}\right),\quad \beta_3 = -\left(\frac{1}{1-\varepsilon_1\theta_\infty}\right),\quad \beta_4 = \left(\frac{\psi+\theta_\infty+\varepsilon_2\theta_{surr}^4}{1-\varepsilon_1\theta_\infty}\right).$$

The leading term will be obtained from the term which is either a constant or a function of the independent variable.

$$\theta_0 = L^{-1}\beta_4 = \int \beta_4 d\tau = \beta_4\tau + c \tag{21}$$

using the initial condition,

$$\theta_0 = 1 + \beta_4\tau \tag{22}$$

The remaining terms may be determined from,

$$\theta_{n+1} = \beta_1 L^{-1}\theta_n \frac{d\theta_n}{d\tau} + \beta_2 L^{-1}\theta_n^4 + \beta_3 L^{-1}\theta_n \tag{25}$$

Representing the non-linear terms with their corresponding Adomian variable, we have:

$$\theta_{n+1} = \beta_1 L^{-1}A[n] + \beta_2 L^{-1}B[n] + \beta_3 L^{-1}\theta_n, \qquad n = 0,1,2,... \tag{26}$$

where the Adomian variables are define as,

$$A[n] = \frac{1}{n!}\frac{d^n}{d\xi^n}\left(\left(\sum_{i=0}^{n}\xi^i\theta[i]\right)^p\left(\sum_{i=0}^{n}\xi^i\frac{d\theta[i]}{d\tau}\right)^q\right) \tag{27a}$$

$$B[n] = \frac{1}{n!}\frac{d^n}{d\xi^n}\left(\sum_{i=0}^{n}\xi^i\theta[i]\right)^r \tag{27b}$$

For the problem at hand, $p = q = 1$ *and* $r = 4$.

For the sake accuracy, 16 Adomian terms were generated for both cases as shown in the Appendix

The term-by-term solutions to the temperature history after incorporating the generated Adomian terms is,

$$\theta_0 = 1 + \left(\frac{\psi + \theta_\infty + \varepsilon_2\theta_{surr}^4}{1 - \varepsilon_1\theta_\infty}\right)\tau \tag{28}$$

$$\theta_1 = \frac{1}{1-\epsilon_1\theta_\infty}\left(\begin{array}{l} -\epsilon_1\left(\dfrac{\tau^2\left(\psi+\epsilon_2\theta_{surr}^4+\theta_\infty\right)^2}{2\left(1-\epsilon_1\theta_\infty\right)^2}+\dfrac{\tau\left(\psi+\epsilon_2\theta_{surr}^4+\theta_\infty\right)}{1-\epsilon_1\theta_\infty}\right)-\tau-\dfrac{\tau^2\left(\psi+\epsilon_2\theta_{surr}^4+\theta_\infty\right)}{2\left(1-\epsilon_1\theta_\infty\right)}- \\ \epsilon_2\left(-\dfrac{1-\epsilon_1\theta_\infty}{5\left(\psi+\epsilon_2\theta_{surr}^4+\theta_\infty\right)}+\dfrac{\left(1-\epsilon_1\theta_\infty\right)\left(1+\dfrac{\tau\left(\psi+\epsilon_2\theta_{surr}^4+\theta_\infty\right)}{1-\epsilon_1\theta_\infty}\right)^5}{5\left(\psi+\epsilon_2\theta_{surr}^4+\theta_\infty\right)}\right) \end{array}\right) \tag{29}$$

$$\theta_2 = \frac{1}{1-\epsilon_1\theta_\infty}\left(\begin{array}{l} -\dfrac{\tau^6\epsilon_2\left(\psi+\epsilon_2\theta_{surr}^4+\theta_\infty\right)^4}{30\left(-1+\epsilon_1\theta_\infty\right)^5}+\dfrac{\tau^5\epsilon_2\left(\psi+\epsilon_2\theta_{surr}^4+\theta_\infty\right)^3}{5\left(-1+\epsilon_1\theta_\infty\right)^4}-\dfrac{\tau^4\epsilon_2\left(\psi+\epsilon_2\theta_{surr}^4+\theta_\infty\right)^2}{2\left(-1+\epsilon_1\theta_\infty\right)^3}- \\ \dfrac{1}{3}\tau^3\left(-\dfrac{\epsilon_1\left(\psi+\epsilon_2\theta_{surr}^4+\theta_\infty\right)^2}{2\left(1-\epsilon_1\theta_\infty\right)^3}-\dfrac{\psi+\epsilon_2\theta_{surr}^4+\theta_\infty}{2\left(1-\epsilon_1\theta_\infty\right)^2}-\dfrac{2\epsilon_2\left(\psi+\epsilon_2\theta_{surr}^4+\theta_\infty\right)}{\left(-1+\epsilon_1\theta_\infty\right)^2}\right)- \\ \dfrac{1}{2}\tau^2\left(-\dfrac{\epsilon_1\left(\psi+\epsilon_2\theta_{surr}^4+\theta_\infty\right)}{\left(1-\epsilon_1\theta_\infty\right)^2}-\dfrac{1}{1-\epsilon_1\theta_\infty}+\dfrac{\epsilon_2}{-1+\epsilon_1\theta_\infty}\right) \end{array}\right) \tag{30}$$

$$\theta_3=\frac{1}{1-\epsilon_1\theta_\infty}\epsilon_1\left(\begin{array}{l}-\frac{\tau\epsilon_1\left(\psi+\epsilon_2\theta_{surr}^4+\theta_\infty\right)}{\left(1-\epsilon_1\theta_\infty\right)^2}-\frac{\tau}{1-\epsilon_1\theta_\infty}-\frac{\tau\epsilon_2}{1-\epsilon_1\theta_\infty}+\frac{1}{6}\tau^6\left(-\frac{\epsilon_2\left(\psi+\epsilon_2\theta_{surr}^4+\theta_\infty\right)^5}{\left(1-\epsilon_1\theta_\infty\right)^6}+\frac{\epsilon_2\left(\psi+\epsilon_2\theta_{surr}^4+\theta_\infty\right)^5}{5\left(1-\epsilon_1\theta_\infty\right)\left(-1+\epsilon_1\theta_\infty\right)^5}\right)+\\ \frac{1}{5}\tau^5\left(-\frac{5\epsilon_2\left(\psi+\epsilon_2\theta_{surr}^4+\theta_\infty\right)^4}{\left(1-\epsilon_1\theta_\infty\right)^5}-\frac{\epsilon_2\left(\psi+\epsilon_2\theta_{surr}^4+\theta_\infty\right)^4}{\left(1-\epsilon_1\theta_\infty\right)\left(-1+\epsilon_1\theta_\infty\right)^4}\right)+\frac{1}{4}\tau^4-\frac{10\epsilon_2\left(\psi+\epsilon_2\theta_{surr}^4+\theta_\infty\right)^3}{\left(1-\epsilon_1\theta_\infty\right)^4}+\frac{2\epsilon_2\left(\psi+\epsilon_2\theta_{surr}^4+\theta_\infty\right)^3}{\left(1-\epsilon_1\theta_\infty\right)\left(-1+\epsilon_1\theta_\infty\right)^3}+\\ \frac{1}{3}\tau^3\left(\begin{array}{l}-\frac{6\epsilon_2\left(\psi+\epsilon_2\theta_{surr}^4+\theta_\infty\right)^2}{\left(1-\epsilon_1\theta_\infty\right)^3}+\frac{\left(\psi+\epsilon_2\theta_{surr}^4+\theta_\infty\right)\left(-\frac{\epsilon_1\left(\psi+\epsilon_2\theta_{surr}^4+\theta_\infty\right)^2}{\left(1-\epsilon_1\theta_\infty\right)^3}+\frac{-\psi-\epsilon_2\theta_{surr}^4-\theta_\infty}{\left(1-\epsilon_1\theta_\infty\right)^2}-\frac{4\epsilon_2\left(\psi+\epsilon_2\theta_{surr}^4+\theta_\infty\right)}{\left(1-\epsilon_1\theta_\infty\right)^2}\right)}{\left(1-\epsilon_1\theta_\infty\right)}+\\ \frac{\left(\psi+\epsilon_2\theta_{surr}^4+\theta_\infty\right)\left(-\frac{\epsilon_1\left(\psi+\epsilon_2\theta_{surr}^4+\theta_\infty\right)^2}{2\left(1-\epsilon_1\theta_\infty\right)^3}-\frac{\psi+\epsilon_2\theta_{surr}^4+\theta_\infty}{2\left(1-\epsilon_1\theta_\infty\right)^2}-\frac{2\epsilon_2\left(\psi+\epsilon_2\theta_{surr}^4+\theta_\infty\right)}{\left(-1+\epsilon_1\theta_\infty\right)^2}\right)}{1-\epsilon_1\theta_\infty}\end{array}\right)+\\ \frac{1}{2}\tau^2\left(\begin{array}{l}-\frac{\epsilon_1\left(\psi+\epsilon_2\theta_{surr}^4+\theta_\infty\right)^2}{\left(1-\epsilon_1\theta_\infty\right)^3}-\frac{\psi+\epsilon_2\theta_{surr}^4+\theta_\infty}{\left(1-\epsilon_1\theta_\infty\right)^2}-\frac{4\epsilon_2\left(\psi+\epsilon_2\theta_{surr}^4+\theta_\infty\right)}{\left(1-\epsilon_1\theta_\infty\right)^2}+\\ \frac{\left(\psi+\epsilon_2\theta_{surr}^4+\theta_\infty\right)}{1-\epsilon_1\theta_\infty}\left(-\frac{2\epsilon_1\left(\psi+\epsilon_2\theta_{surr}^4+\theta_\infty\right)}{\left(1-\epsilon_1\theta_\infty\right)^2}-\frac{2}{1-\epsilon_1\theta_\infty}-\frac{\epsilon_2}{1-\epsilon_1\theta_\infty}+\frac{\epsilon_2}{-1+\epsilon_1\theta_\infty}\right)\end{array}\right)\end{array}\right) \tag{31}$$

Following the definition of ADM, the general solution is:

$$\theta(\tau)=\sum_{j=0}^{n}\theta_j=\theta_0+\theta_1+\theta_2+\theta_3+\theta_4+\theta_5+\theta_6+\theta_7+...+\theta_n$$

4. Results and discussion

Table 1 depicts the verification of the analytical scheme used with a numerical forth order Runge-Kutta. A good agreement with the numerical method was obtained.

Table. 1
Comparison of ADM results with a numerical method for a 20μm iron particle

τ	θ (τ) for a Particle diameter of (μm)	
	Numerical	**ADM**
0.0	1.000000000000000	1.000000000000000
0.1	1.113333969181095	1.113333981177264
0.2	1.215117348008129	1.215117711150980
0.3	1.306590963764452	1.306593345739770
0.4	1.388844932815013	1.388852820269113
0.5	1.462843666959360	1.462858827578177
0.6	1.529449065177065	1.529458070391791
0.7	1.589444597054137	1.589387100510296
0.8	1.643562984179010	1.643271057270020
0.9	1.692520185796611	1.691615617727115
1.0	1.737058395009000	1.734792471017498

4.1. Effect of particle diameter on the temperature profile

Fig. 2 depicts the effect of the combusting particle diameter on temperature profile and burning rate. From the graphs, it can be easily seen that particle diameter has evident influence on the temperature profile. A particle with 60μm diameter was observed to possess a higher temperature profile which means that an increase in the combusting particle diameter causes a corresponding increase in the temperature profile as well as the burning time. As a result of this evident impact, the particle diameter may be used as a controlling agent in reducing the hazardous effects that normally propagate from iron particle combustion.

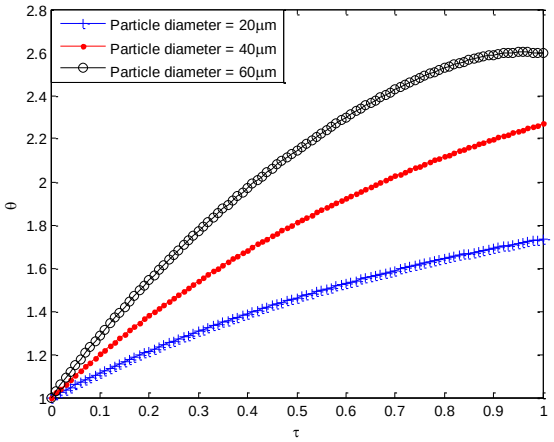

Fig. 2. Effect of particle diameter on the temperature Profile with ADM

4.2. Effect of ε_1 and ε_2 on the temperature profile

Fig. 3 and Fig. 4 depict the influence of ε_1 and ε_2 on the temperature profile. From the figures, it can be seen that increasing ε_1 and ε_2 decreases the combustion temperature with this effect more pronounced with ε_2. The decrease in combustion temperature with a corresponding increase in ε_1 and ε_2 is as a result of an increase in the radiation heat transfer term in the combustion particle.

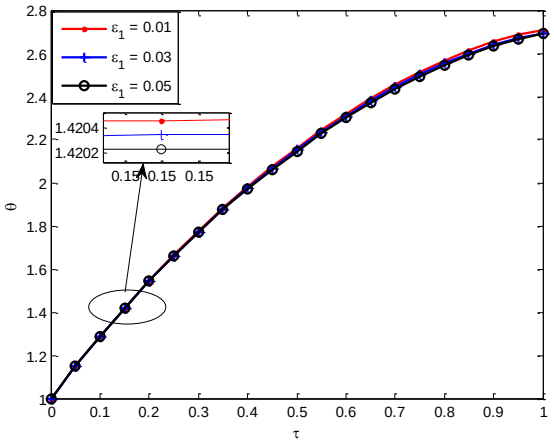

Fig. 3. Effect of ε_1 on the temperature profile.

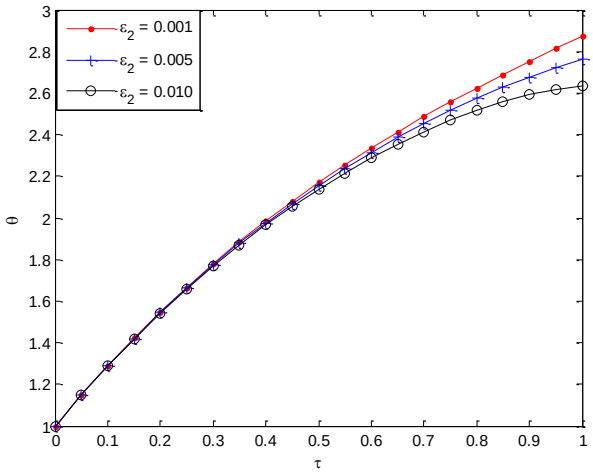

Fig. 4. Effect of ε_2 on the temperature profile.

4.3. Effect of the heat realized parameter and surrounding temperature on the temperature profile

Fig. 5 and Fig. 6 depict the influence of the heat realized parameter and the surrounding temperature on the combustion temperature. From the plots, we can conclude that increasing the heat realized parameter and the surrounding temperature increases the combustion temperature. This increase is significant for the heat realized parameter variation than that of the surrounding temperatures except for high values of surrounding temperature.

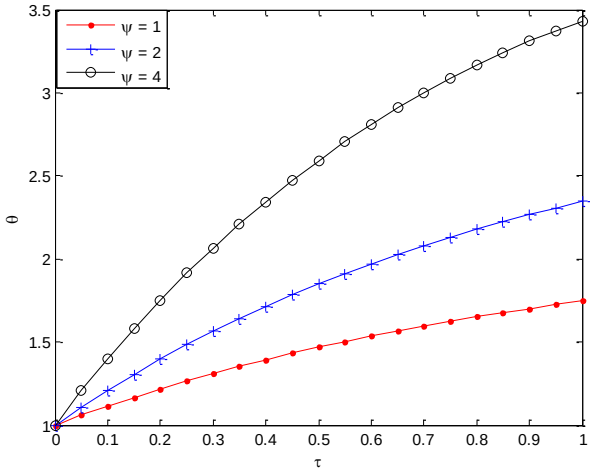

Fig. 5. Effect of heat realized term on the temperature profile.

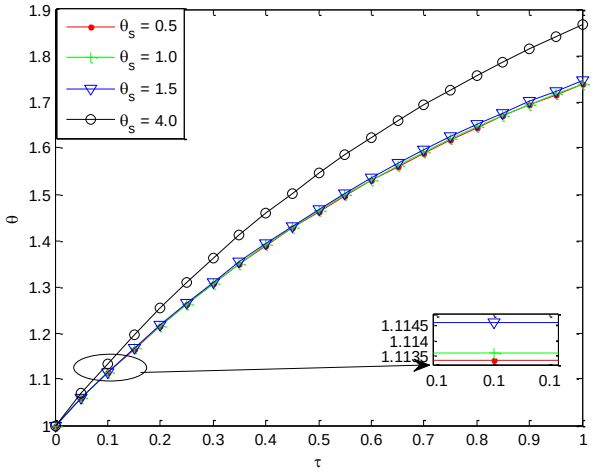

Fig. 6. Effect of surrounding temperature on the temperature profile.

5. Conclusion

In this work, Adomian decomposition method has been used to developed analytical solution to transient combustion analysis for iron micro-particles in a gaseous oxidizing medium. The results of the ADM were verified numerically. Also, parametric studies were performed to fully understand how the combusting particle diameter, density, radiative term, heat realized term and other parameters affect the burning time as well as the combustion temperature. The results revealed that by increasing the heat realized parameter, combustion temperature increased until a steady state was reached. It is hoped that the present study will enhance the understanding of the combustion of the particle and also obviate the challenges facing industries on combustion of metallic particles such as iron particles as well as in the determination of different particles burning time.

References

[1] Sun J-H, Dobashi R, Hirano T. Combustion Behavior of Iron Particles Suspended in Air. Combust Sci Technol 2000;150:99–114. doi:10.1080/00102200008952119.

[2] Haghiri A, Bidabadi M. Dynamic behavior of particles across flame propagation through micro-iron dust cloud with thermal radiation effect. Fuel 2011;90:2413–21. doi:10.1016/j.fuel.2011.03.032.

[3] Liu Y, Sun J, Chen D. Flame propagation in hybrid mixture of coal dust and methane. J Loss Prev Process Ind 2007;20:691–7. doi:10.1016/j.jlp.2007.04.029.

[4] Bidabadi M, Haghiri A, Rahbari A. Mathematical modeling of velocity and number density profiles of particles across the flame propagation through a micro-iron dust cloud. J Hazard Mater 2010;176:146–53. doi:10.1016/j.jhazmat.2009.10.130.

[5] Haghiri A, Bidabadi M. Modeling of laminar flame propagation through organic dust cloud with thermal radiation effect. Int J Therm Sci 2010;49:1446–56. doi:10.1016/j.ijthermalsci.2010.03.013.

[6] Hatami M, Ganji DD, Boubaker K. Temperature Variations Analysis for Condensed Matter Micro- and Nanoparticles Combustion Burning in Gaseous Oxidizing Media by DTM and BPES. ISRN Condens Matter Phys 2013;2013:1–8. doi:10.1155/2013/129571.

[7] Bidabadi M, Mafi M. Time variation of combustion temperature and burning time of a single iron particle. Int J Therm Sci 2013;65:136–47. doi:10.1016/j.ijthermalsci.2012.10.019.

[8] Stern RH, Rasmussen H. Left ventricular ejection: Model solution by collocation, an approximate analytical method. Comput Biol Med 1996;26:255–61. doi:10.1016/0010-4825(96)00007-8.

[9] Vaferi B, Salimi V, Dehghan Baniani D, Jahanmiri A, Khedri S. Prediction of transient pressure response in the petroleum reservoirs using orthogonal collocation. J Pet Sci Eng 2012;98–99:156–63. doi:10.1016/j.petrol.2012.04.023.

[10] Hatami M, Hasanpour A, Ganji DD. Heat transfer study through porous fins (Si3N4 and AL) with temperature-dependent heat generation. Energy Convers Manag 2013;74:9–16. doi:10.1016/j.enconman.2013.04.034.

[11] Bouaziz MN, Aziz A. Simple and accurate solution for convective–radiative fin with temperature dependent thermal conductivity using double optimal linearization. Energy Convers Manag 2010;51:2776–82. doi:10.1016/j.enconman.2010.05.033.

[12] Aziz A, Bouaziz MN. A least squares method for a longitudinal fin with temperature dependent internal heat generation and thermal conductivity. Energy Convers Manag 2011;52:2876–82. doi:10.1016/j.enconman.2011.04.003.

[13] Shaoqin G, Huoyuan D. Negative norm least-squares methods for the incompressible magnetohydrodynamic equations. Acta Math Sci 2008;28:675–84. doi:10.1016/S0252-9602(08)60069-7.

[14] Hatami M, Nouri R, Ganji DD. Forced convection analysis for MHD Al2O3–water nanofluid flow over a horizontal plate. J Mol Liq 2013;187:294–301. doi:10.1016/j.molliq.2013.08.008.

[15] Hatami M, Sheikholeslami M, Ganji DD. Laminar flow and heat transfer of nanofluid between contracting and rotating disks by least square method. Powder Technol 2014;253:769–79. doi:10.1016/j.powtec.2013.12.053.

[16] Hatami M, Hatami J, Ganji DD. Computer simulation of MHD blood conveying gold nanoparticles as a third grade non-Newtonian nanofluid in a hollow porous vessel. Comput Methods Programs Biomed 2014;113:632–41. doi:10.1016/j.cmpb.2013.11.001.

[17] Hatami M, Ganji DD. Thermal performance of circular convective–radiative porous fins with different section shapes and materials. Energy Convers Manag 2013;76:185–93. doi:10.1016/j.enconman.2013.07.040.

[18] Hatami M, Ganji DD. Heat transfer and nanofluid flow in suction and blowing process between parallel disks in presence of variable magnetic field. J Mol Liq 2014;190:159–68. doi:10.1016/j.molliq.2013.11.005.

[19] Hatami M, Ganji DD. Natural convection of sodium alginate (SA) non-Newtonian nanofluid flow between two vertical flat plates by analytical and numerical methods. Case Stud Therm Eng 2014;2:14–22. doi:10.1016/j.csite.2013.11.001.

[20] Hatami M, Domairry G. Transient vertically motion of a soluble particle in a Newtonian fluid media. Powder Technol 2014;253:481–5. doi:10.1016/j.powtec.2013.12.015.

[21] Domairry G, Hatami M. Squeezing Cu–water nanofluid flow analysis between parallel plates by DTM-Padé Method. J Mol Liq 2014;193:37–44. doi:10.1016/j.molliq.2013.12.034.

[22] Ahmadi AR, Zahmatkesh A, Hatami M, Ganji DD. A comprehensive analysis of the flow and heat transfer for a nanofluid over an unsteady stretching flat plate. Powder Technol 2014;258:125–33. doi:10.1016/j.powtec.2014.03.021.

[23] Saedodin S, Shahbabaei M. Thermal Analysis of Natural Convection in Porous Fins with Homotopy Perturbation Method (HPM). Arab J Sci Eng 2013;38:2227–31. doi:10.1007/s13369-013-0581-6.

[24] Darvishi MT, Gorla RSR, Khani F, Aziz A. Thermal performance of a porus radial fin with natural convection and radiative heat losses. Therm Sci 2015;19:669–78.

[25] Moradi A, Hayat T, Alsaedi A. Convection-radiation thermal analysis of triangular porous fins with temperature-dependent thermal conductivity by DTM. Energy Convers Manag 2014;77:70–7. doi:10.1016/j.enconman.2013.09.016.

[26] Hoshyar H, Ganji DD, Abbasi M. Determination of temperature distribution for porous fin with temperature-dependent heat generation by homotopy analysis method. J Appl Mech Eng 2015;4:153.

[27] Adomian G. Solving frontier problems of physics: the decomposition method. vol. 60. Springer Science & Business Media; 2013.

[28] Adomian G. A review of the decomposition method in applied mathematics. J Math Anal Appl 1988;135:501–44. doi:10.1016/0022-247X(88)90170-9.

[29] Haldar K. Application of Adomian's approximations to the Navier-Stokes equations in cylindrical coordinates. Appl Math Lett 1996;9:109–13. doi:10.1016/0893-9659(96)00061-4.

[30] Chiu C-H, Chen C-K. A decomposition method for solving the convective longitudinal fins with variable thermal conductivity. Int J Heat Mass Transf 2002;45:2067–75. doi:10.1016/S0017-9310(01)00286-1.

[31] Adomian G. Solution of the Thomas–Fermi equation, Appl. Math. Lett 1998;11:31–133.

[32] Adomian G. Analytical solution of Navier-Stokes flow of a viscous compressible fluid. Found Phys Lett 1995;8:389–400.

[33] Arora HL, Abdelwahid FI. Solution of non-integer order differential equations via the Adomian decomposition method. Appl Math Lett 1993;6:21–3.

[34] Momani S. A decomposition method for solving unsteady convection-diffusion problems. Turkish J Math 2008;32:51–60.

[35] Ganji DD, Sheikholeslami M, Ashorynejad HR. Analytical approximate solution of nonlinear differential equation governing Jeffery-Hamel flow with high magnetic field by Adomian decomposition method. Int Sch Res Not 2011;2011.

[36] Haldar K. Application of Adomian's approximation to blood flow through arteries in the presence of a magnetic field. J Appl Math Comput 2003;12:267–79. doi:10.1007/BF02936199.

[37] Makinde OD, Olajuwon BI, Gbolagade AW. Adomian decomposition approach to a boundary layer flow with thermal radiation past a moving vertical porous plate. Int J Appl Math Mech 2007;3:62–70.

[38] Somali S, Gokmen G. Adomian decomposition method for nonlinear Sturm-Liouville problems. Surv Math Its Appl 2007;2:11–20.

Appendix

The Adomian polynomials for the first non-linear terms are

$$A_0 = \theta_0 \dot{\theta}_0$$

$$A_1 = \theta_0 \dot{\theta}_1 + \theta_1 \dot{\theta}_0$$

$$A_2 = \theta_0 \dot{\theta}_2 + \theta_1 \dot{\theta}_1 + \theta_2 \dot{\theta}_0$$

$$A_3 = \theta_0 \dot{\theta}_3 + \theta_1 \dot{\theta}_2 + \theta_2 \dot{\theta}_1 + \theta_3 \dot{\theta}_0$$

$$A_4 = \theta_0 \dot{\theta}_4 + \theta_4 \dot{\theta}_0 + \theta_2 \dot{\theta}_2 + \theta_1 \dot{\theta}_3 + \theta_3 \dot{\theta}_1$$

$$A_5 = \theta_0 \dot{\theta}_5 + \theta_5 \dot{\theta}_0 + \theta_4 \dot{\theta}_1 + \theta_1 \dot{\theta}_4 + \theta_2 \dot{\theta}_3 + \theta_3 \dot{\theta}_2$$

$$A_6 = \theta_5 \dot{\theta}_1 + \theta_4 \dot{\theta}_2 + \theta_3 \dot{\theta}_3 + \theta_2 \dot{\theta}_4 + \theta_0 \dot{\theta}_6 + \theta_6 \dot{\theta}_0 + \theta_1 \dot{\theta}_5$$

$$A_7 = \theta_4 \dot{\theta}_3 + \theta_3 \dot{\theta}_4 + \theta_1 \dot{\theta}_6 + \theta_6 \dot{\theta}_1 + \theta_2 \dot{\theta}_5 + \theta_0 \dot{\theta}_7 + \theta_7 \dot{\theta}_0 + \theta_5 \dot{\theta}_2$$

$$A_8 = \theta_8 \dot{\theta}_0 + \theta_0 \dot{\theta}_8 + \theta_5 \dot{\theta}_3 + \theta_4 \dot{\theta}_4 + \theta_2 \dot{\theta}_6 + \theta_6 \dot{\theta}_2 + \theta_3 \dot{\theta}_5 + \theta_1 \dot{\theta}_7 + \theta_7 \dot{\theta}_1$$

$$A_9 = \theta_8 \dot{\theta}_1 + \theta_1 \dot{\theta}_8 + \theta_5 \dot{\theta}_4 + \theta_3 \dot{\theta}_6 + \theta_6 \dot{\theta}_3 + \theta_2 \dot{\theta}_7 + \theta_7 \dot{\theta}_2 + \theta_4 \dot{\theta}_5 + \theta_0 \dot{\theta}_9 + \theta_9 \dot{\theta}_0$$

$$A_{10} = \theta_0 \dot{\theta}_{10} + \theta_{10} \dot{\theta}_0 + \theta_8 \dot{\theta}_2 + \theta_2 \dot{\theta}_8 + \theta_5 \dot{\theta}_5 + \theta_4 \dot{\theta}_6 + \theta_6 \dot{\theta}_4 + \theta_7 \dot{\theta}_3 + \theta_3 \dot{\theta}_7 + \theta_9 \dot{\theta}_1 + \theta_1 \dot{\theta}_9$$

$$A_{11} = \theta_1 \dot{\theta}_{10} + \theta_{10} \dot{\theta}_1 + \theta_8 \dot{\theta}_3 + \theta_3 \dot{\theta}_8 + \theta_5 \dot{\theta}_6 + \theta_6 \dot{\theta}_5 + \theta_7 \dot{\theta}_4 + \theta_4 \dot{\theta}_7 + \theta_9 \dot{\theta}_2 + \theta_2 \dot{\theta}_9 + \theta_0 \dot{\theta}_{11} + \theta_{11} \dot{\theta}_0$$

$$A_{12} = \theta_{11} \dot{\theta}_1 + \theta_0 \dot{\theta}_{12} + \theta_2 \dot{\theta}_{10} + \theta_{10} \dot{\theta}_2 + \theta_8 \dot{\theta}_4 + \theta_6 \dot{\theta}_6 + \theta_7 \dot{\theta}_5 + \theta_5 \dot{\theta}_7 + \theta_9 \dot{\theta}_3 + \theta_3 \dot{\theta}_9 + \theta_4 \dot{\theta}_8 + \theta_1 \dot{\theta}_{11} + \theta_{12} \dot{\theta}_0$$

$$A_{13} = \theta_8 \dot{\theta}_5 + \theta_7 \dot{\theta}_6 + \theta_6 \dot{\theta}_7 + \theta_9 \dot{\theta}_4 + \theta_4 \dot{\theta}_9 + \theta_5 \dot{\theta}_8 + \theta_2 \dot{\theta}_{11} + \theta_{12} \dot{\theta}_1 + \theta_0 \dot{\theta}_{13} + \theta_{13} \dot{\theta}_0 + \theta_1 \dot{\theta}_{12} + \theta_{11} \dot{\theta}_2 + \theta_3 \dot{\theta}_{10} + \theta_{10} \dot{\theta}_3$$

$$A_{14} = \theta_2 \dot{\theta}_{12} + \theta_{11} \dot{\theta}_3 + \theta_4 \dot{\theta}_{10} + \theta_{10} \dot{\theta}_4 + \theta_6 \dot{\theta}_8 + \theta_8 \dot{\theta}_6 + \theta_7 \dot{\theta}_7 + \theta_9 \dot{\theta}_5 + \theta_5 \dot{\theta}_9 + \theta_3 \dot{\theta}_{11} + \theta_{12} \dot{\theta}_2 + \theta_1 \dot{\theta}_{13} + \theta_{13} \dot{\theta}_1 + \theta_0 \dot{\theta}_{14} + \theta_{14} \dot{\theta}_0$$

$$A_{15} = \theta_{14} \dot{\theta}_1 + \theta_5 \dot{\theta}_{10} + \theta_{10} \dot{\theta}_5 + \theta_7 \dot{\theta}_8 + \theta_8 \dot{\theta}_7 + \theta_9 \dot{\theta}_6 + \theta_6 \dot{\theta}_9 + \theta_4 \dot{\theta}_{11} + \theta_{12} \dot{\theta}_3 + \theta_2 \dot{\theta}_{13} + \theta_{13} \dot{\theta}_2 + \theta_1 \dot{\theta}_{14} + \theta_0 \dot{\theta}_{15} + \theta_{15} \dot{\theta}_0 + \theta_3 \dot{\theta}_{12} + \theta_{11} \dot{\theta}_4$$

$$A_{16} = \theta_1 \dot{\theta}_{15} + \theta_{15} \dot{\theta}_1 + \theta_4 \dot{\theta}_{12} + \theta_{11} \dot{\theta}_5 + \theta_6 \dot{\theta}_{10} + \theta_{10} \dot{\theta}_6 + \theta_8 \dot{\theta}_8 + \theta_9 \dot{\theta}_7 + \theta_7 \dot{\theta}_9 + \theta_{12} \dot{\theta}_4 + \theta_3 \dot{\theta}_{13} + \theta_{13} \dot{\theta}_3 + \theta_5 \dot{\theta}_{11} + \theta_0 \dot{\theta}_{16} + \theta_{16} \dot{\theta}_0 + \theta_2 \dot{\theta}_{14} + \theta_{14} \dot{\theta}_2$$

Also, the Adomian polynomials for the second non-linear terms are

$$B_0 = \theta_0^4$$

$$B_1 = 4\theta_0^3\theta_1$$

$$B_2 = 4\theta_0^3\theta_2 + 6\theta_0^2\theta_1^2$$

$$B_3 = 4\theta_0^3\theta_3 + 12\theta_0^2\theta_1\theta_2 + 4\theta_0\theta_1^3$$

$$B_4 = 4\theta_0^3\theta_4 + 12\theta_0^2\theta_1\theta_3 + 6\theta_0^2\theta_2^2 + 12\theta_0\theta_1^2\theta_2 + \theta_1^4$$

$$B_5 = 4\theta_0^3\theta_5 + 12\theta_0^2\theta_1\theta_4 + 12\theta_0^2\theta_2\theta_3 + 12\theta_0\theta_1^2\theta_3 + 12\theta_0\theta_1\theta_2^2 + 4\theta_1^3\theta_2$$

$$B_6 = 4\theta_0^3\theta_6 + 12\theta_0^2\theta_1\theta_5 + 12\theta_0^2\theta_2\theta_4 + 6\theta_0^2\theta_3^2 + 12\theta_0\theta_1^2\theta_4 + 24\theta_0\theta_1\theta_2\theta_3 + 4\theta_0\theta_2^3 + 4\theta_1^3\theta_3 + 6\theta_1^2\theta_2^2$$

$$B_7 = 4\theta_0^3\theta_7 + 12\theta_0^2\theta_1\theta_6 + 12\theta_0^2\theta_2\theta_5 + 12\theta_0^2\theta_3\theta_4 + 12\theta_0\theta_1^2\theta_5 + 24\theta_0\theta_1\theta_2\theta_4 + 12\theta_0\theta_1\theta_3^2 + 12\theta_0\theta_2^2\theta_3 + 4\theta_1^3\theta_4 + 12\theta_1^2\theta_2\theta_3 + 4\theta_1\theta_2^3$$

$$B_8 = 4\theta_0^3\theta_8 + 12\theta_0^2\theta_1\theta_7 + 12\theta_0^2\theta_2\theta_6 + 12\theta_0^2\theta_3\theta_5 + 6\theta_0^2\theta_4^2 + 12\theta_0\theta_1^2\theta_6 + 24\theta_0\theta_1\theta_2\theta_5 + 24\theta_0\theta_1\theta_3\theta_4 + 12\theta_0\theta_2^2\theta_4 + 12\theta_0\theta_2\theta_3^2 + 4\theta_1^3\theta_5 + 12\theta_1^2\theta_2\theta_4 + 6\theta_1^2\theta_3^2 + 12\theta_1\theta_2^2\theta_3 + \theta_2^4$$

$$B_9 = 4\theta_0^3\theta_9 + 12\theta_0^2\theta_1\theta_8 + 12\theta_0^2\theta_2\theta_7 + 12\theta_0^2\theta_3\theta_6 + 12\theta_0^2\theta_4\theta_5 + 12\theta_0\theta_1^2\theta_7 + 24\theta_0\theta_1\theta_2\theta_6 + 24\theta_0\theta_1\theta_3\theta_5 + 12\theta_0\theta_1\theta_4^2 + 12\theta_0\theta_2^2\theta_5 + 24\theta_0\theta_2\theta_3\theta_4 + 4\theta_0\theta_3^3 + 4\theta_1^3\theta_6 + 12\theta_1^2\theta_2\theta_5 + 12\theta_1^2\theta_3\theta_4 + 12\theta_1\theta_2^2\theta_4 + 12\theta_1\theta_2\theta_3^2 + 4\theta_2^3\theta_3$$

$$B_{10} = 4\theta_0^3\theta_{10} + 12\theta_0^2\theta_1\theta_9 + 12\theta_0^2\theta_2\theta_8 + 12\theta_0^2\theta_3\theta_7 + 12\theta_0^2\theta_4\theta_6 + 6\theta_0^2\theta_5^2 + 12\theta_0\theta_1^2\theta_8 + 24\theta_0\theta_1\theta_2\theta_7 + 24\theta_0\theta_1\theta_3\theta_6 + 24\theta_0\theta_1\theta_4\theta_5 + 12\theta_0\theta_2^2\theta_6 + 24\theta_0\theta_2\theta_3\theta_5 + 12\theta_0\theta_2\theta_4^2 + 12\theta_0\theta_3^2\theta_4 + 4\theta_1^3\theta_7 + 12\theta_1^2\theta_2\theta_6 + 12\theta_1^2\theta_3\theta_5 + 6\theta_1^2\theta_4^2 + 12\theta_1\theta_2^2\theta_5 + 24\theta_1\theta_2\theta_3\theta_4 + 4\theta_1\theta_3^3 + 4\theta_2^3\theta_4 + 6\theta_2^2\theta_3^2$$

$$B_{11} = 4\theta_0^3\theta_{11} + 12\theta_0^2\theta_1\theta_{10} + 12\theta_0^2\theta_2\theta_9 + 12\theta_0^2\theta_3\theta_8 + 12\theta_0^2\theta_4\theta_7 + 12\theta_0^2\theta_5\theta_6 + 12\theta_0\theta_1^2\theta_9 + 24\theta_0\theta_1\theta_2\theta_8 + 24\theta_0\theta_1\theta_3\theta_7 + 24\theta_0\theta_1\theta_4\theta_6 + 12\theta_0\theta_1\theta_5^2 + 12\theta_0\theta_2^2\theta_7 + 24\theta_0\theta_2\theta_3\theta_6 + 24\theta_0\theta_2\theta_4\theta_5 + 12\theta_0\theta_3^2\theta_5 + 12\theta_0\theta_3\theta_4^2 + 4\theta_1^3\theta_8 + 12\theta_1^2\theta_2\theta_7 + 12\theta_1^2\theta_3\theta_6 + 12\theta_1^2\theta_4\theta_5 + 12\theta_1\theta_2^2\theta_6 + 24\theta_1\theta_2\theta_3\theta_5 + 12\theta_1\theta_2\theta_4^2 + 12\theta_1\theta_3^2\theta_4 + 4\theta_2^3\theta_5 + 12\theta_2^2\theta_3\theta_4 + 4\theta_2\theta_3^3$$

$$B_{12} = 4\theta_0^3\theta_{12} + 12\theta_0^2\theta_1\theta_{11} + 12\theta_0^2\theta_2\theta_{10} + 12\theta_0^2\theta_3\theta_9 + 12\theta_0^2\theta_4\theta_8 + 12\theta_0^2\theta_5\theta_7 + 6\theta_0^2\theta_6^2 + 12\theta_0\theta_1^2\theta_{10} + 24\theta_0\theta_1\theta_2\theta_9 + 24\theta_0\theta_1\theta_3\theta_8 + 24\theta_0\theta_1\theta_4\theta_7 + 24\theta_0\theta_1\theta_5\theta_6 + 12\theta_0\theta_2^2\theta_8 + 24\theta_0\theta_2\theta_3\theta_7 + 24\theta_0\theta_2\theta_4\theta_6 + 12\theta_0\theta_2\theta_5^2 + 12\theta_0\theta_3^2\theta_6 + 24\theta_0\theta_3\theta_4\theta_5 + 4\theta_0\theta_4^3 + 4\theta_1^3\theta_9 + 12\theta_1^2\theta_2\theta_8 + 12\theta_1^2\theta_3\theta_7 + 12\theta_1^2\theta_4\theta_6 + 6\theta_1^2\theta_5^2 + 12\theta_1\theta_2^2\theta_7 + 24\theta_1\theta_2\theta_3\theta_6 + 24\theta_1\theta_2\theta_4\theta_5 + 12\theta_1\theta_3^2\theta_5 + 12\theta_1\theta_3\theta_4^2 + 4\theta_2^3\theta_6 + 12\theta_2^2\theta_3\theta_5 + 6\theta_2^2\theta_4^2 + 12\theta_2\theta_3^2\theta_4 + \theta_3^4$$

$$B_{13} = 4\theta_0^3\theta_{13} + 12\theta_0^2\theta_1\theta_{12} + 12\theta_0^2\theta_2\theta_{11} + 12\theta_0^2\theta_3\theta_{10} + 12\theta_0^2\theta_4\theta_9 + 12\theta_0^2\theta_5\theta_8 + 12\theta_0^2\theta_6\theta_7 + 12\theta_0\theta_1^2\theta_{11} + 24\theta_0\theta_1\theta_2\theta_{10} + 24\theta_0\theta_1\theta_3\theta_9 + 24\theta_0\theta_1\theta_4\theta_8 + 24\theta_0\theta_1\theta_5\theta_7 + 12\theta_0\theta_1\theta_6^2 + 12\theta_0\theta_2^2\theta_9 + 24\theta_0\theta_2\theta_3\theta_8 + 24\theta_0\theta_2\theta_4\theta_7 + 24\theta_0\theta_2\theta_5\theta_6 + 12\theta_0\theta_3^2\theta_7 + 24\theta_0\theta_3\theta_4\theta_6 + 12\theta_0\theta_3\theta_5^2 + 12\theta_0\theta_4^2\theta_5 + 4\theta_1^3\theta_{10} + 12\theta_1^2\theta_2\theta_9 + 12\theta_1^2\theta_3\theta_8 + 12\theta_1^2\theta_4\theta_7 + 12\theta_1^2\theta_5\theta_6 + 12\theta_1\theta_2^2\theta_8 + 24\theta_1\theta_2\theta_3\theta_7 + 24\theta_1\theta_2\theta_4\theta_6 + 12\theta_1\theta_2\theta_5^2 + 12\theta_1\theta_3^2\theta_6 + 24\theta_1\theta_3\theta_4\theta_5 + 4\theta_1\theta_4^3 + 4\theta_2^3\theta_7 + 12\theta_2^2\theta_3\theta_6 + 12\theta_2^2\theta_4\theta_5 + 12\theta_2\theta_3^2\theta_5 + 12\theta_2\theta_3\theta_4^2 + 4\theta_3^3\theta_4$$

$$B_{14} = 4\theta_0^3\theta_{14} + 12\theta_0^2\theta_1\theta_{13} + 12\theta_0^2\theta_2\theta_{12} + 12\theta_0^2\theta_3\theta_{11} + 12\theta_0^2\theta_4\theta_{10} + 12\theta_0^2\theta_5\theta_9 + 12\theta_0^2\theta_6\theta_8 + 6\theta_0^2\theta_7^2 + 12\theta_0\theta_1^2\theta_{12} + 24\theta_0\theta_1\theta_2\theta_{11} + 24\theta_0\theta_1\theta_3\theta_{10} + 24\theta_0\theta_1\theta_4\theta_9 + 24\theta_0\theta_1\theta_5\theta_8 + 24\theta_0\theta_1\theta_6\theta_7 + 12\theta_0\theta_2^2\theta_{10} + 24\theta_0\theta_2\theta_3\theta_9 + 24\theta_0\theta_2\theta_4\theta_8 + 24\theta_0\theta_2\theta_5\theta_7 + 12\theta_0\theta_2\theta_6^2 + 12\theta_0\theta_3^2\theta_8 + 24\theta_0\theta_3\theta_4\theta_7 + 24\theta_0\theta_3\theta_5\theta_6 + 12\theta_0\theta_4^2\theta_6 + 12\theta_0\theta_4\theta_5^2 + 4\theta_1^3\theta_{11} + 12\theta_1^2\theta_2\theta_{10} + 12\theta_1^2\theta_3\theta_9 + 12\theta_1^2\theta_4\theta_8 + 12\theta_1^2\theta_5\theta_7 + 6\theta_1^2\theta_6^2 + 12\theta_1\theta_2^2\theta_9 + 24\theta_1\theta_2\theta_3\theta_8 + 24\theta_1\theta_2\theta_4\theta_7 + 24\theta_1\theta_2\theta_5\theta_6 + 12\theta_1\theta_3^2\theta_7 + 24\theta_1\theta_3\theta_4\theta_6 + 12\theta_1\theta_3\theta_5^2 + 12\theta_1\theta_4^2\theta_5 + 4\theta_2^3\theta_8 + 12\theta_2^2\theta_3\theta_7 + 12\theta_2^2\theta_4\theta_6 + 6\theta_2^2\theta_5^2 + 12\theta_2\theta_3^2\theta_6 + 24\theta_2\theta_3\theta_4\theta_5 + 4\theta_2\theta_4^3 + 4\theta_3^3\theta_5 + 6\theta_3^2\theta_4^2$$

$$B_{15} = 4\theta_0^3\theta_{15} + 12\theta_0^2\theta_1\theta_{14} + 12\theta_0^2\theta_2\theta_{13} + 12\theta_0^2\theta_3\theta_{12} + 12\theta_0^2\theta_4\theta_{11} + 12\theta_0^2\theta_5\theta_{10} + 12\theta_0^2\theta_6\theta_9 + 12\theta_0^2\theta_7\theta_8 + 12\theta_0\theta_1^2\theta_{13} + 24\theta_0\theta_1\theta_2\theta_{12} + 24\theta_0\theta_1\theta_3\theta_{11} + 24\theta_0\theta_1\theta_4\theta_{10} + 24\theta_0\theta_1\theta_5\theta_9 + 24\theta_0\theta_1\theta_6\theta_8 + 12\theta_0\theta_1\theta_7^2 + 12\theta_0\theta_2^2\theta_{11} + 24\theta_0\theta_2\theta_3\theta_{10} + 24\theta_0\theta_2\theta_4\theta_9 + 24\theta_0\theta_2\theta_5\theta_8 + 24\theta_0\theta_2\theta_6\theta_7 + 12\theta_0\theta_3^2\theta_9 + 24\theta_0\theta_3\theta_4\theta_8 + 24\theta_0\theta_3\theta_5\theta_7 + 12\theta_0\theta_3\theta_6^2 + 12\theta_0\theta_4^2\theta_7 + 24\theta_0\theta_4\theta_5\theta_6 + 4\theta_0\theta_5^3 + 4\theta_1^3\theta_{12} + 12\theta_1^2\theta_2\theta_{11} + 12\theta_1^2\theta_3\theta_{10} + 12\theta_1^2\theta_4\theta_9 + 12\theta_1^2\theta_5\theta_8 + 12\theta_1^2\theta_6\theta_7 + 12\theta_1\theta_2^2\theta_{10} + 24\theta_1\theta_2\theta_3\theta_9 + 24\theta_1\theta_2\theta_4\theta_8 + 24\theta_1\theta_2\theta_5\theta_7 + 12\theta_1\theta_2\theta_6^2 + 12\theta_1\theta_3^2\theta_8 + 24\theta_1\theta_3\theta_4\theta_7 + 24\theta_1\theta_3\theta_5\theta_6 + 12\theta_1\theta_4^2\theta_6 + 12\theta_1\theta_4\theta_5^2 + 4\theta_2^3\theta_9 + 12\theta_2^2\theta_3\theta_8 + 12\theta_2^2\theta_4\theta_7 + 12\theta_2^2\theta_5\theta_6 + 12\theta_2\theta_3^2\theta_7 + 24\theta_2\theta_3\theta_4\theta_6 + 12\theta_2\theta_3\theta_5^2 + 12\theta_2\theta_4^2\theta_5 + 4\theta_3^3\theta_6 + 12\theta_3^2\theta_4\theta_5 + 4\theta_3\theta_4^3$$

$$B_{16} = 4\theta_0^3\theta_{16} + 12\theta_0^2\theta_1\theta_{15} + 12\theta_0^2\theta_2\theta_{14} + 12\theta_0^2\theta_3\theta_{13} + 12\theta_0^2\theta_4\theta_{12} + 12\theta_0^2\theta_5\theta_{11} + 12\theta_0^2\theta_6\theta_{10} + 12\theta_0^2\theta_7\theta_9 + 6\theta_0^2\theta_8^2 + 12\theta_0\theta_1^2\theta_{14} + 24\theta_0\theta_1\theta_2\theta_{13} + 24\theta_0\theta_1\theta_3\theta_{12} + 24\theta_0\theta_1\theta_4\theta_{11} + 24\theta_0\theta_1\theta_5\theta_{10} + 24\theta_0\theta_1\theta_6\theta_9 + 24\theta_0\theta_1\theta_7\theta_8 + 12\theta_0\theta_2^2\theta_{12} + 24\theta_0\theta_2\theta_3\theta_{11} + 24\theta_0\theta_2\theta_4\theta_{10} + 24\theta_0\theta_2\theta_5\theta_9 + 24\theta_0\theta_2\theta_6\theta_8 + 12\theta_0\theta_2\theta_7^2 + 12\theta_0\theta_3^2\theta_{10} + 24\theta_0\theta_3\theta_4\theta_9 + 24\theta_0\theta_3\theta_5\theta_8 + 24\theta_0\theta_3\theta_6\theta_7 + 12\theta_0\theta_4^2\theta_8 + 24\theta_0\theta_4\theta_5\theta_7 + 12\theta_0\theta_4\theta_6^2 + 12\theta_0\theta_5^2\theta_6 + 4\theta_1^3\theta_{13} + 12\theta_1^2\theta_2\theta_{12} + 12\theta_1^2\theta_3\theta_{11} + 12\theta_1^2\theta_4\theta_{10} + 12\theta_1^2\theta_5\theta_9 + 12\theta_1^2\theta_6\theta_8 + 6\theta_1^2\theta_7^2 + 12\theta_1\theta_2^2\theta_{11} + 24\theta_1\theta_2\theta_3\theta_{10} + 24\theta_1\theta_2\theta_4\theta_9 + 24\theta_1\theta_2\theta_5\theta_8 + 24\theta_1\theta_2\theta_6\theta_7 + 12\theta_1\theta_3^2\theta_9 + 24\theta_1\theta_3\theta_4\theta_8 + 24\theta_1\theta_3\theta_5\theta_7 + 12\theta_1\theta_3\theta_6^2 + 12\theta_1\theta_4^2\theta_7 + 24\theta_1\theta_4\theta_5\theta_6 + 4\theta_1\theta_5^3 + 4\theta_2^3\theta_{10} + 12\theta_2^2\theta_3\theta_9 + 12\theta_2^2\theta_4\theta_8 + 12\theta_2^2\theta_5\theta_7 + 6\theta_2^2\theta_6^2 + 12\theta_2\theta_3^2\theta_8 + 24\theta_2\theta_3\theta_4\theta_7 + 24\theta_2\theta_3\theta_5\theta_6 + 12\theta_2\theta_4^2\theta_6 + 12\theta_2\theta_4\theta_5^2 + 4\theta_3^3\theta_7 + 12\theta_3^2\theta_4\theta_6 + 6\theta_3^2\theta_5^2 + 12\theta_3\theta_4^2\theta_5 + \theta_4^4$$